



Ocean acidification, warming and feeding impacts on biomineralization pathways and shell material properties of *Magallana gigas* and *Mytilus* spp.

Isabella Mele^a, Rona A.R. McGill^b, Jordan Thompson^a, James Fennell^a, Susan Fitzer^{a,*}

^a Institute of Aquaculture, University of Stirling, Stirling, FK94LA, United Kingdom

^b Stable Isotope Ecology Lab, Scottish Universities Environmental Research Centre, University of Glasgow, Glasgow, G75 0QF, United Kingdom

ABSTRACT

Molluscs are among the organisms affected by ocean acidification (OA), relying on carbon for shell biomineralization. Metabolic and environmental sourcing are two pathways potentially affected by OA, but the circumstances and patterns by which they are altered are poorly understood. From previous studies, mollusc shells grown under OA appear smaller in size, brittle and thinner, suggesting an important alteration in carbon sequestration. However, supplementary feeding experiments have shown promising results in offsetting the negative consequences of OA on shell growth. Our study compared carbon uptake by $\delta^{13}\text{C}$ tracing and deposition into mantle tissue and shell layers in *Magallana gigas* and *Mytilus* species, two economically valuable and common species. After subjecting the species to 7.7 pH, +2 °C seawater, and enhanced feeding, both species maintain shell growth and metabolic pathways under OA without benefitting from extra feeding, thus, showing effective acclimation to rapid and short-term environmental change. *Mytilus* spp. increases metabolic carbon into the calcite and environmental sourcing of carbon into the shell aragonite in low pH and high temperature conditions. Low pH affects *M. gigas* mantle nitrogen isotopes maintaining growth. Calcite biomineralization pathway differs between the two species and suggests species-specific response to OA.

1. Introduction

Climate change and ocean acidification (OA), induced by rising atmospheric carbon dioxide (CO_2), are global phenomena which threaten marine organisms biomineralizing calcium carbonate (CaCO_3) shells. The average ocean acidity is expected to decrease by 0.14–0.43 units, with a simultaneous increase of +2 °C and +4 °C in sea surface temperature by 2100 (Hoegh-Guldberg et al., 2014). Consequently, the seawater bicarbonate (HCO_3^-) and carbonic acid (H_2CO_3) equilibrium is affected (Waldbusser et al., 2015; Lee et al., 2021) causing under-saturation of oceanic calcite and aragonite worldwide: predicted with “very high confidence” (IPCC et al., 2018). This scenario is already present in upwelling zones in the Northern America, Northern Mexico (Feely et al., 2008), and polar regions (Jones et al., 2017) where CaCO_3 saturation decreases below horizon level. As the ocean’s pH decreases, the extent of the effect of OA is dependent on the shell structure and composition of the organism (Fitzer et al., 2018; Gazeau et al., 2007). Calcium carbonate can present most commonly as one of two polymorphs, calcite being the stable hexagonal form, and aragonite being considered metastable and more vulnerable to OA (Chandler, 2015). Both *Mytilus* species (spp.) and *Magallana gigas* form calcite layers, but *Mytilus* spp. also forms aragonite on the inner shell layer. Although the two polymorphs share the same chemical formula, the different atomic

arrangement of aragonite increases susceptibility to OA, compared to calcite (Jones et al., 2017). Consequences such as shell dissolution and corrosion indeed result in physiological weaknesses affecting economic viability of molluscs for human consumption.

$\delta^{13}\text{C}$ and $\delta^{15}\text{N}$ are two isotopic signatures that are used to accredit carbon and nitrogen sourcing. $\delta^{13}\text{C}$ is a ratio of carbon-13 and carbon-12 stable isotopes which can be used to understand the route of dissolved inorganic carbon. In seawater geochemistry $\delta^{13}\text{C}$ can be used to determine anthropogenic pollution from both atmosphere and riverine inputs, under OA for example, addition of CO_2 results in a lower $\delta^{13}\text{C}$ (Lee et al., 2021; Fitzer et al., 2018; 2019a). In biology and for bivalves respired CO_2 is often depleted in heavier carbon isotope as these biological processes favour uptake of the lower mass isotope through kinetic fractionation. Therefore $\delta^{13}\text{C}$ in bivalves can be used to trace carbon deposited in biological tissues such as the mantle after feeding and respiration, or in the shell via the periostracum, and fluid and pericellular pathways (McConnaughey and Gillikin, 2008). A lower $\delta^{13}\text{C}$ value in biological tissue denotes a metabolic mobilisation, and in bivalve shell analyses, low $\delta^{13}\text{C}$ indicates carbon acquisition from environmental sourcing.

On the other hand, $\delta^{15}\text{N}$ is used as a signature in food web patterns, where high values are directly related to upper trophic levels and high nutrient inputs, such as during eutrophication (Bearhop et al., 2004;

* Corresponding author.

E-mail address: susan.fitzer@stir.ac.uk (S. Fitzer).

<https://doi.org/10.1016/j.marenvres.2023.105925>

Received 25 August 2022; Received in revised form 10 February 2023; Accepted 17 February 2023

Available online 19 February 2023

0141-1136/© 2023 The Authors. Published by Elsevier Ltd. This is an open access article under the CC BY license (<http://creativecommons.org/licenses/by/4.0/>).

Perkins et al., 2014; Carmichael et al., 2012). Assimilation of $\delta^{15}\text{N}$ in bivalves is also used as a proxy to assess nutrient affluence and primary producers' presence in ecosystems, allowing identification of terrestrial nitrogen input into marine environments (Lake et al., 2001; Howard et al., 2005). Elevated $\delta^{15}\text{N}$ deposition in bivalves can be attributed to enhanced nitrogen input from catchments or terrestrial systems, feeding patterns, or anaerobic metabolism during starvation in low-oxygen conditions (Howard et al., 2005; Patterson and Carmichael, 2018). Aging and large size also result in increased $\delta^{15}\text{N}$ deposition in bivalve tissue (Howard et al., 2005).

Mytilus spp. and *Magallana gigas* together account for 46% of global mollusc production within the aquaculture industry (Wijsman et al., 2018). Previous research has investigated the importance of extra feed source in *M. edulis* (Lee et al., 2021), and genetic variability and selection in *S. glomerata* (Fitzer et al., 2019a) as tools to reverse the potential negative effects of OA. Indeed, gene expression for biomineralization control is influenced by stress-responses because of insufficient food availability under OA, but after providing extra feed, shell properties in *M. edulis* have been restored to control-levels (Lee et al., 2021). Previous research has shown that increasing food supply to molluscs during OA experiments can limit shell corrosion (Melzner et al., 2011) and increase shell growth (Thomsen et al., 2013). CO_2 induced OA has been shown to increase phytoplankton growth and lipid concentrations in *Isochrysis galbana*, a key aquaculture feed species (Fitzer et al., 2019b). Therefore, there is potential to enhance food and nutrient availability for molluscs under OA.

It has been hypothesised that metabolic carbon uptake from food overtakes environmental intake in biomineralization, under OA, as more energy is required to maintain acid-base homeostasis and sustain growth (Sanders et al., 2018; Clark, 2020), but this response has been observed only in *M. edulis* (Lee et al., 2021). Indeed, the mechanisms by which carbon uptake affects shell and growth remain unclear. Metabolic and environmental uptake are the two mechanisms by which *Mytilus* spp. acquire carbon for biomineralization, but the conditions in which one subsidises the other are also poorly understood (Fitzer et al., 2019a). So far, OA-driven shell abnormalities have been linked to changes in intracellular and extracellular homeostasis (Hamm et al., 2015), energy metabolism, protein stability and enzymatic activity (Pörtner H.-O., 2008; Tomanek et al., 2011). Shifts in metabolic mobilisation of carbon have been observed under OA in *M. edulis* (Lee et al., 2021), causing brittle and misshapen shells (Gaylord et al., 2011), reduced shell thickness index, and structural changes (Fitzer et al., 2015b; Castillo et al., 2017). At the same time, it is unclear whether OA responses are innate to species, or if other non-species-specific factors are applicable on a global scale. Given the different shell CaCO_3 polymorph composites in the two families, this study focuses on a comparative analysis of *Magallana gigas* and *Mytilus* spp. as two economically valuable species. In general, within UK waters there is a *Mytilus* spp. complex present, comprising of mostly *Mytilus edulis*, hybridised with *Mytilus galloprovincialis* and very few ($\sim <4\%$) *Mytilus trossulus*. So, this study reports the genus as a reference for locally tested hybrids in the area of collection (Carboni et al., 2021).

Thus, for the first time, this study tests the mixed effects of pH, temperature, and feeding regime on carbon sequestration, shell growth and properties of both *M. gigas* and *Mytilus* spp., containing different polymorph composites, calcite only and aragonite and calcite respectively. The aim is to identify the pathways of mobilisation and disruption of carbon uptake and transfer in *Mytilus* spp. and *M. gigas*, and the potential resultant changes in shell mechanical properties in an experimental comparative approach. Extra feed is implemented to evaluate the potential for OA-induced algae growth to act as an effective nutrient enrichment in an OA farming scenario to enable continued biomineralization in *Mytilus* spp. and *M. gigas*.

2. Materials and methods

Mytilus hybrids and *M. gigas* were supplied by Loch Fyne Oysters Ltd at the same age of harvest ~ 2 years.

2.1. Experimental design

The experimental treatments were conducted at the Marine Environmental Research Laboratory (MERL), University of Stirling. Prior to experimental acclimation, each individual mollusc was individually labelled using plastic numbers stuck to the shell with araldite, 8 molluscs were placed into each 10 L replicate tank (8 treatments, 64 experimental tanks and 512 molluscs in total). Both species were acclimated (ambient conditions, 12°C , pH 8.1) from the 8th of November until the November 13, 2021 before altering any environmental variable. The conditions were changed over the course of 1 day. The treatments continued for 36 days, finishing on the December 18, 2021. There were eight experimental treatments, examining the interactive effects of pH (8.1 versus 7.7), temperature (12°C versus 14°C) and feeding (Control versus extra feed) in a full factorial experimental design. The system recirculated water from a 400 L sump for each treatment in a closed system, however, no filtration was used as a complete water change occurred every other day and was sufficient to avoid detritus build up.

The control pH and seawater temperature follow seasonal values at the time of the experiment (November and December) and the experimental treatments for pH (7.7) and temperature ($+2^\circ\text{C}$) reflect IPCC predicted environmental conditions for 2100 (IPCC et al., 2021). Seawater was warmed from 12°C to 14°C using 200 W tank heaters. The pH was measured daily in each tank using a Aquamedic pH probe in NBS scale and adjusted using the Aquamedic pH computer via solenoid valve release of CO_2 . The Aquamedic pH probes were brand new at the start of the experiment and did not have any bio fouling, which has been shown previously to potentially impact pH probes over long term use. Before and during the experimental period, the probes were regularly checked for fouling, cleaned, and calibrated, as mentioned in other experimental procedures (Fitzer et al., 2019a). In addition, pH was checked separately with a pHmeter and regularly calibrated for each tank.

Temperature, pH, and salinity were recorded daily, and seawater samples were collected weekly, filtered, and stored for carbon analyses.

Average seawater carbonate chemistry parameters were collected per each tank and averaged by treatment group (Table 1). The mean water temperature, salinity, pH, and $\delta^{13}\text{C}$ are also paired with calculated pCO_2 values. The DIC was measured using filtered water samples and show that each treatment did change as expected to represent future ocean acidification scenarios for carbonate chemistry. In the case of pH, because of a particularly low pH measurement in tank treatments 28–32 (Table 1), standardised pH values are also displayed.

The feeding consists of a standard aquarium plankton feed with 25% *Isochrysis galbana*, 20% Pavlova sp., 20% *Tetraselmis suecica*, 15% *Thalassiosira weissflogii*, 20% Nannochloropsis spp. (Fitzer et al., 2015a). The mix feed was provided to the animals daily, with algae concentrations recorded weekly. Two drops of feed were fed to all control tanks, with an average concentration of $\sim 8 \times 10^6$ cells/ml, four drops of feed were fed to all extra feed tanks, with a concentration of $\sim 16 \times 10^6$ cells/ml. There were no other differences between the algae feeds, the same feed stock was used for all tanks.

Each labelled mollusc was weighed, and measured for length, depth and width of shell using a calliper at the start and end of experimental acclimation. For all analyses, four animals were sampled for each experimental treatment, one per each of the four replicate tanks, in total 32 *Mytilus* samples and 32 *M. gigas* individuals. Each mollusc was euthanized by placing on ice, and then dissected to separate the mantle tissue from the shell. The same labelled individual mollusc was used for mantle and shell isotope analysis, and shell property assessment.

Table 1

Seawater pCO₂ was calculated using CO2SYS. Seawater measured parameters include temperature, pH, salinity, DIC in δ¹³C VPDB as per Riebesell et al. (2010). For temperature and salinity average values with standard deviation are reported by replicate variations. Calculations are obtained from two samples per tank, in total eight measurements per treatment.

Feeding(million cells/ml)	Temperature(°C)	pH(standard)	pH(averaged)	Salinity(PSU)	δ ¹³ C(‰)	pCO ₂ (µatm)	Tank replicates(n)
8	11.45 ± 0.86	8.1	7.91 ± 0.08	28.42 ± 4.07	-1.49	506	1–4
8	11.7 ± 0.84	7.7	7.71 ± 0.07	32.78 ± 1.42	-5.49	826	5–8
16	11.55 ± 0.87	8.1	7.95 ± 0.15	28.42 ± 4.07	-1.76	661	9–12
16	11.8 ± 0.85	7.7	7.67 ± 0.13	36.1 ± 3.84	-6.56	951	13–16
8	13.65 ± 1.03	8.1	7.96 ± 0.09	36.58 ± 3.84	-1.57	521	17–20
8	13.6 ± 1.03	7.7	7.72 ± 0.93	36.1 ± 3.84	-2.67	800	21–24
16	13.55 ± 1.07	8.1	7.81 ± 0.11	36.58 ± 3.84	-3.77	584	28–32
16	13.7 ± 1.02	7.7	7.73 ± 0.13	36.1 ± 3.84	-5.97	821	33–36

2.2. Shell isotope analysis preparation

The shell samples were visually examined for any biofilm trace, rinsed, and cleaned with a plastic brush, and left to air dry. Then, 2 mg of calcite powder was manually sampled off the shell's new growth margins. Shell powders were obtained using a diamond tipped etching pen to remove only the surface of the calcite/aragonite without contaminating between the two polymorphs. This is possible due to aragonite and calcite being visually distinguishable allowing for separation by etching ventral and dorsal sides to separate the layers, according to the natural coloration of the two polymorphs. A fine (~10 µm) surface layer was removed to collect the required ~1 mg of powder for each shell. Individual molluscs were labelled and measured at the start and end of the experiment, to determine the new growth in mm. We were then able to collect samples for the outer ~2 mm of the shells to ensure the sampling of only new growth. Then, 0.7–1.5 mg of calcite powder from each individual mollusc was weighed using a microbalance to four decimal places (OHAUS Pioneer PX224). A micro spatula was used to transfer the powder from tin foil sheets to glass vials. The procedure is identical for *Mytilus* spp. and *M. gigas* shell isotope samples, with both calcite and aragonite were sampled from the *Mytilus* spp.' shell margins.

2.3. Mantle tissue isotope analysis preparation

The mantle samples were selected to match the equivalent shell sample ID from the batch. The aim was to have shell and tissue powder from the same organism for comparison and analysis purposes. The biological samples were dissected at MERL and placed in 1.5 ml Eppendorf tubes stored at -18 °C. The corresponding mantle tissue samples were freeze-dried in a SciQuip Alpha 1-4LSC model, with 1.030mBar vacuum, +20 °C shelf temperature, and -63 °C ice condition. The freeze-drier ran for a minimum of 18 h, up to 24 h per batch. The samples were then homogenised using a pestle and mortar. Using a micro spatula, 0.7–1.5 mg dried powder was weighed into tin capsules for isotope analyses.

2.4. Isotope analysis

VPDB δ¹³C and δ¹⁵N isotopes of organic C and N from mantle tissue were analysed at the Scottish Universities Environmental Research Centre (SUERC) in the Stable Isotope Ecology Lab, using continuous flow isotope ratio mass spectroscopy (Elementar vario-Pyrocube, Elemental Analyser interfaced with a Thermo Fisher Scientific, Delta Plus XP, Mass Spectrometer) as per Fitzer et al. (2019a). Shell carbon isotope analysis of inorganic carbon was measured using an AP 2003 continuous flow automated carbonate system, with results reported as Fitzer et al. (2019a).

2.5. Shell preparation for microindentation

As per Fitzer et al. (2015a), the left valve of the *Mytilus* spp. was embedded in 70 g of clear epoxy resin in silicone moulds according to

their experimental treatments. For *M. gigas*, all the left cupped valves were placed in upright identical position on the silicone moulds. As per Fitzer et al. (2015b), the shell samples were embedded in epoxy resin for a minimum of 24 h, sliced longitudinally, perpendicular to the opening hinge, with a diamond edged abrasive Isomet 500 saw, and hand polished for 2–4 min per each sandpaper grit using circular sandpaper (P240, P600, P1200, P2500, P4000).

Micro indentation was performed to measure microhardness. Vicker's hardness micro-indentation (Leco Vickers LM 248AT micro-indentation hardness tester) method was completed as per Fitzer et al. (2015b). 10–12 diamond shaped indents were performed on each dry shell, applying a force of 0.3 kg for 10 s. The indents were performed ~30 µm (approximately the diameter of one indent) from the most external visible layer of shell material, at intervals of at least 30 µm from one another to ensure no overlap between indents. For each polished shell sample D1, D2 and HV/hardness were recorded. Results were collected for *Mytilus* spp. calcite and *M. gigas* calcite, and averaged across each individual shell sample.

2.6. Shell thickness index (STI)

STI is a method of Freeman and Byers (2006), determined for the dried shell samples (n = 4) for each environmental treatment. As per equation:

$$STI = \frac{1000 * \text{Shell Weight}}{\left[\text{Length} * (\text{Height}^2 + \text{Width}^2)^{0.5} \right] * \frac{\pi}{2}}$$

A digital electronic calliper was used on the dried shells to take the measurements. The weight of the dried shells was taken using a mass balance. In the case of STI measurements a high STI indicated a thicker shell, whilst a low STI indicates a thinner shell (Fitzer et al., 2015b).

2.7. Statistical analysis

Data analysis used a Mixed Effects Model for isotope values in relationship with the environmental factors and feeding regime across *Mytilus* spp. and *M. gigas*. The model is used to test whether there is an alteration of δ¹³C, and δ¹⁵N in shell and organic tissue according to the different treatments, food regime, temperatures, and pH levels. The fixed factors are established as temperature, pH, and feeding regime; the isotope values represent the response variable, while the treatment is a random factor. Mixed Effects Models are also applied to STI, HV, and growth data in terms of mass, depth, length, and width to assess the significance of the fixed effect. All statistical analyses are conducted with RStudio version 4.1.1 with packages tidyverse, MuMIn, lme4, and lmerTest.

All statistical assumptions were tested, and none violated. Diagnostics test includes Residual vs Fitted plot, Normal Q-Q plot, Scale Location plot and Residual VS Leverage Cook's distance.

A student T-T test was also conducted in R 4.1.1 for comparing means between groups.

3. Results

3.1. Metabolic carbon

3.1.1. $\delta^{13}\text{C}$ in mantle tissue

Overall, the measurements of average carbon isotope values in the mantle tissue of *M. gigas* and *Mytilus* spp. follow a similar trend. The average $\delta^{13}\text{C}$ of *Mytilus* spp. mantle tissues was significantly different from that of *M. gigas* tissues (Unpaired Two-Sample T-Test, $p = 2.2 \times 10^{-16}$), with *M. gigas* mantle tissues having significantly lower carbon isotope values compared to *Mytilus* spp. mantle tissues (Fig. 1). A linear trend is present in both *Mytilus* spp. and *M. gigas*, with a decrease in median carbon isotope values for both groups for treatment four (pH = 7.7, Extra feeding regime, ambient temperature), and six (pH = 7.7, Control feeding, increased temperature +2 °C).

3.1.2. $\delta^{15}\text{N}$ isotope in mantle tissue

Nitrogen isotopes values for *M. gigas* mantle tissues were higher than in *Mytilus* spp. mantle tissues (Fig. 2). Mixed effect analysis of temperature, pH, and feeding regime with random treatment effect does not highlight any relevant significance in $\delta^{15}\text{N}$ values for *Mytilus* spp. ($p > 0.05$, Table S10).

For *M. gigas*, the Mixed Effect Model shows a significant influence of pH on mantle $\delta^{15}\text{N}$ ($p = 0.048$, Table S11). In acidified conditions, $\delta^{15}\text{N}$ values were lower in the mantle tissues. Although the trend is more visually distinct in ambient 12 °C, the increase of temperature does not significantly affect the results (Table S11).

3.2. Environmental carbon

The $\delta^{13}\text{C}$ values in calcite shell samples show significant variance from the mean between *Mytilus* spp. and *M. gigas* (F - Test, $p = 9.3 \times 10^{-4}$), Table S12). *M. gigas* $\delta^{13}\text{C}$ shell calcite does not respond significantly to changes of environmental factors or feeding throughout the treatments ($p > 0.05$, Table S13).

Mytilus spp. $\delta^{13}\text{C}$ mean calcite and aragonite values are significantly different among the treatments (Unpaired Two-Sample T-Test, $p = 1.2 \times 10^{-5}$), Table S14). Carbon isotope values in shell aragonite shows different trends and mean values to shell calcite. Overall, the lowest carbon isotope values are reported in aragonite, while calcite shows significantly higher means (Fig. 3).

Carbon isotope measurements are significantly affected by the effect of pH in the treatments, this applies both in the case of calcite and

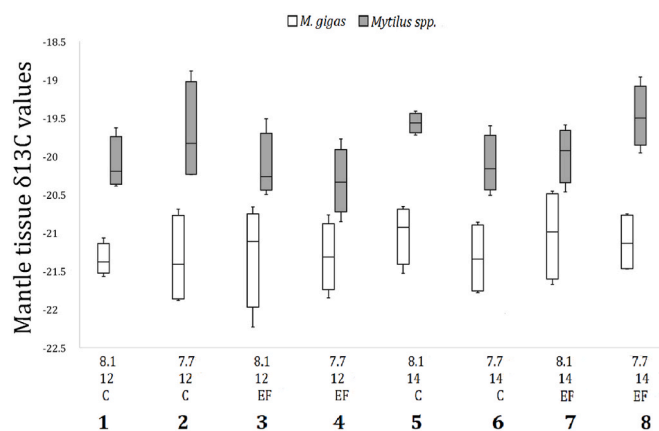


Fig. 1. $\delta^{13}\text{C}$ values compared for *Mytilus* spp. (Grey bars) and *M. gigas* (White bars) mantle tissue displayed as a boxplot. Each treatment is described top to bottom with pH (8.1, 7.7), temperature (°C), and feeding regime (C = control, EF = Extra Feeding). Mixed effects models marks no significant influence of either pH, temperature or feeding regime on mantle tissue $\delta^{13}\text{C}$ (Supplementary Tables S6–9).

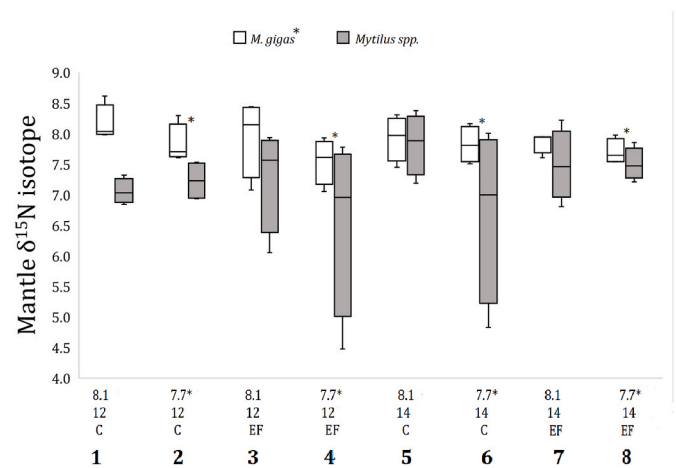


Fig. 2. $\delta^{15}\text{N}$ results in *Mytilus* spp. (grey bars) and *M. gigas* (white bars) mantle tissue displayed as a boxplot. Each treatment is described top to bottom with pH (8.1, 7.7), temperature (°C), and feeding regime (C = control, EF = Extra Feeding). * denotes significance, mixed effects models marks a significant effect of low pH (pH 7.7) on *M. gigas* $\delta^{15}\text{N}$ (Mean $\delta^{15}\text{N}$ 8.079 ± 0.120‰, $t = 2.065$, $p = 0.048$).

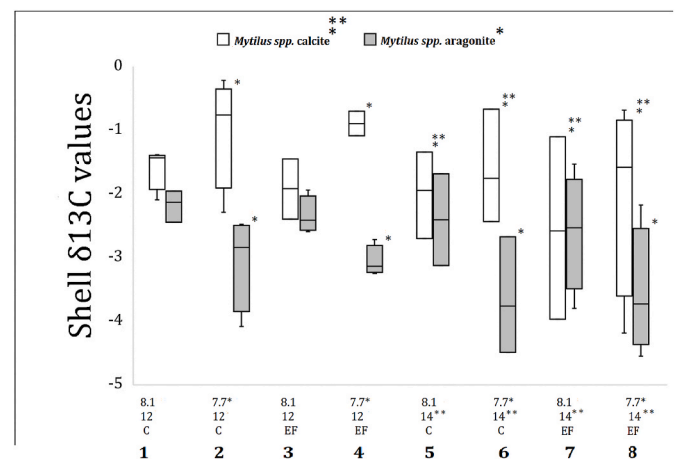


Fig. 3. *Mytilus* spp. $\delta^{13}\text{C}$ results for calcite (White bars) and aragonite (Grey bars) displayed as a boxplot. Each treatment is described top to bottom with pH (8.1, 7.7), temperature (°C), and feeding regime (C = control, EF = Extra Feeding). * denotes significance, mixed effects models marks a significant effect of low pH (mean $\delta^{13}\text{C}$ -1.713 ± 0.352‰, $t = -2.398$, $p = 0.0254$) and ** for increased temperature (mean $\delta^{13}\text{C}$ -1.5739 ± 0.339‰, $t = -2.081$, $p = 0.049$) in calcite and * for low pH only in aragonite (mean $\delta^{13}\text{C}$ -2.111 ± 0.261‰, $t = 3.150$, $p = 0.004$).

aragonite ($p = 0.025$ and $p = 0.004$ respectively, Table S15, Table S16). However, the two polymorphs have opposite trends. While aragonite shows significantly lower $\delta^{13}\text{C}$ values in acidified conditions, calcite $\delta^{13}\text{C}$ values are higher in the same environmental conditions. Also, calcite $\delta^{13}\text{C}$ is affected by the change in temperature across treatments, resulting in overall lower $\delta^{13}\text{C}$ values in +2 °C conditions ($p = 0.049$, Table S15).

3.3. Shell growth and mechanical properties

Both *M. gigas* and *Mytilus* spp. shell growth data (Tables S4 and S5) is recorded in terms of depth, length, width, and mass across the experimental treatments. Shell thickness and shell hardness are also reported accordingly (Tables S4 and S5). In the case of *Mytilus* spp., the hardness results refer to calcite only for comparison purposes with *M. gigas*.

In the case of *M. gigas*, none of the growth and shell property parameters is affected by pH, temperature, or feeding conditions ($p > 0.05$, Table S17–20, S26, and S28). Similarly, shell hardness and all the growth measurements of *Mytilus* spp. are not affected by treatment changes in the experiment ($p > 0.05$, Table S21–24, and S27). However, the thickness of *Mytilus* spp. shell is positively influenced by the changes of temperature ($p = 0.023$, Table S25). Median values and quartile ranges are higher in $+2\text{ }^{\circ}\text{C}$ conditions than in control temperature treatments (Fig. 4).

4. Discussion

Patterns of alteration in $\delta^{13}\text{C}$ values can be reflected in shell mechanical properties when the compensation mechanisms under OA are not sufficient to sustain normal growth and physiological functioning. In other words, any significant results in terms of shell material properties suggest a direct response to OA conditions, when also accompanied by changes in carbon mobilisation through the mantle in the shell (Lee et al., 2019). At the same time, compromised shell growth has been identified in conjunction with disordered crystallography linked to insufficient energy acquisition from metabolic pathways (Fitzer et al., 2019a). Therefore, a comparative analysis of metabolic and environmental carbon sequestration dynamics would outline taxon-specific trends or intraspecific consequences of OA.

4.1. $\delta^{15}\text{N}$ and algal feed trends under OA

Assessing the changes and impacts of algal feed from food web interactions is important to understand the role and influence of nutrients and energy sourcing in molluscs under OA. Nevertheless, algal feed provides essential unsaturated fatty acids of key importance in optimal physiological functioning in *Mytilus* spp. and other organisms (Fitzer et al., 2019b). A significant alteration in nitrogen isotope values denotes an important variation in feeding for *M. gigas* (Lafrancois et al., 2018). In this study, lower $\delta^{15}\text{N}$ values in acidified conditions indicate a shift in feeding patterns in *M. gigas*. This is relatable to a physiological and metabolic response to OA conditions. In this study, the implementation of extra feeding does not alter the $\delta^{15}\text{N}$ deposition into the mantle tissue and no growth parameter is compromised, suggesting that *M. gigas* may consume more algae under low pH, potentially explaining the efficient

maintenance of shell growth throughout the treatments. Nitrogen is an essential nutrient for algae, and changes in nitrogen isotopic values can highlight changes in algal productivity (Montoya, 2007). Specifically, $\delta^{15}\text{N}$ is analysed in relation to the nitrogen cycle equilibrium of nutrients in marine and terrestrial ecosystems (Robinson, 2001). $\delta^{15}\text{N}$ of marine zooplankton can be used as an index for the transfer of nitrogen through a food web, from microalgae to *Mytilus* spp. and *M. gigas* by noting the tissue relative enrichment of nitrogen to its food source (Montoya, 2007). An increase in $\delta^{15}\text{N}$ in real-world scenarios has been linked to a proportional increase in $\delta^{15}\text{N}$ in macrophytes species (Cole et al., 2004).

The algae species used in this experiment are primary producers and the ultimate food source for *M. gigas* and *Mytilus* spp. As this is a short-term feeding experiment, the precise relationship between algal feed and overall nitrogen data needs further study. Although OA and increased pCO_2 could affect algal concentration and productivity, total lipids, fatty acids, sterols, LCAs, and alkenoates content in *I. galbana* decrease under OA conditions (Fitzer et al., 2019b). However, OA-related nutrient alterations in algal feed species have been poorly studied so far, and recent OA experiments suggest changes in algae concentrations and fatty acids are species-specific (Fitzer et al., 2019b), thus, for this study, it is difficult to distinguish the concentration specific to species, given that several species were used as feed.

4.2. Metabolic $\delta^{13}\text{C}$ pathways

For carbon sourced metabolically in the mantle (Lee et al., 2021; Fitzer et al., 2014), this study suggests that there is no marked difference in the carbon uptake or biomineralization pathway between *Mytilus* spp. and *M. gigas* (Fig. 1).

An increase in metabolic carbon mobilisation in *M. edulis* has been previously observed by Lee et al. (2021), with less DIC available under OA biomineralization balanced by increasing metabolic carbon uptake. Whilst mantle tissue in *Mytilus* spp. was not significantly altered in low pH conditions, shell calcite $\delta^{13}\text{C}$ were significantly higher. For shell carbonates, $\delta^{13}\text{C}$ of less than -1‰ indicates that CO_3^{2-} is the source of carbon, whereas between -1‰ and $+1\text{‰}$ indicates HCO_3^- as a source of carbon (potentially metabolic; Fitzer et al., 2019a). In *Mytilus* spp. the aragonite becomes lower in $\delta^{13}\text{C}$ following acidified seawater DIC, below -1‰ indicates that CO_3^{2-} is the source of carbon from an environmental route into the shell (Fitzer et al., 2019a). In contrast the calcite is higher in $\delta^{13}\text{C}$ under low pH treatment, above -1‰ indicating HCO_3^- as a source of carbon (potentially metabolic; Fitzer et al., 2019a), although not supported in the mantle tissue $\delta^{13}\text{C}$, this could be metabolically sourced at the extrapallial fluid, but further analyses would be required to determine this. Indeed, this study supports such findings with changes in shell calcite $\delta^{13}\text{C}$, as pCO_2 decreases significantly when pH drops below control conditions, suggesting an overall decrease in environmental carbon availability, consequently, metabolic carbon is mobilised from the mantle to the shell to sustain biomineralization (McConnaughey and Gillikin, 2008). Such a trend is considered to represent an altered metabolic pathway. Other OA studies on *M. edulis* have confirmed the metabolic resilience and adaptation to balance stressful environmental conditions. Matoo et al. (2021) have seen significant metabolic resilience under moderate OA scenarios in 100–300 years future prediction scenarios. Physio-metabolic adaptation has been attributed to the innate resilience of the Mytilids family, as ancestral evolutionary mechanisms promote shell growth and hardness under adverse environmental conditions, such as low pH (Beniash et al., 2010; Beesley et al., 2008).

The reliance on metabolically sourced carbon proves to be an effective strategy to maintain shell growth as depth, width, and length. In this study there was no significant difference in growth under OA conditions, consequently, the metabolic carbon mobilisation pathway is sufficient to sustain *Mytilus* spp. shell growth under moderate OA. Extra feed has not been shown, in this study, to play an important role in promoting resilience, contrasting other studies (Hettinger et al., 2013;

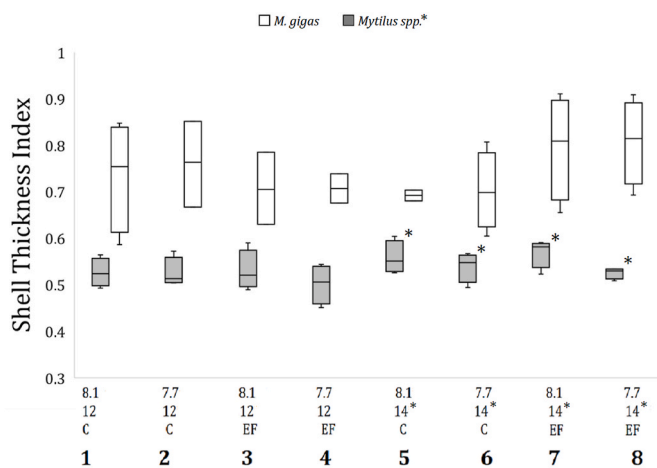


Fig. 4. The Shell Thickness Index (STI) in *Mytilus* spp. (grey bars) and *M. gigas* (white bars) displayed as a boxplot. Each treatment is described top to bottom with pH (8.1, 7.7), temperature ($^{\circ}\text{C}$), and feeding regime (C = control, EF = Extra Feeding). * denotes significance, mixed effects models marks a significant effect of increased temperature on STI (mean STI -0.619 ± 0.021 , $t = 2.402$, $p = 0.023$). *M. gigas* shows an overall thicker shell than *Mytilus* spp., an increase in STI is consistent across $+2\text{ }^{\circ}\text{C}$ in *Mytilus* spp. measurements.

Thomsen et al., 2013). Also, according to this study, OA has no significant effect on shell calcite, shown by STI and hardness data. Lee et al. (2021) observed that extra feed provided enough metabolically sourced carbon to restore shell growth to control levels, supporting our observation that with the provision of extra feed *Mytilus* spp. calcite indeed shows a stable thickness index throughout the experiments (Fig. 4). In this study, calcite analysis was prioritised over aragonite as it is comparable between the two species, both containing calcite in equivalent experimental conditions. But in further investigations, aragonite trends could also be assessed in a thoughtful study of Mytilids.

Given the short duration of the study, a longer treatment period could highlight precise patterns and alter the significance of mantle. For example, Lee et al. (2021) observed that during four months in OA conditions, metabolic $\delta^{13}\text{C}$ of *M. edulis* was compromised, but then restored to control levels after the fourth month threshold. An increase in metabolic carbon mobilisation in *M. edulis* is attributed to less DIC available under OA, balanced by increasing metabolic carbon uptake (Lee et al., 2021). With low pCO_2 and an overall decrease in environmental carbon availability, metabolic carbon is mobilised from the mantle to the shell to sustain biomineralization (McConnaughey and Gillikin, 2008).

For *M. gigas*, the changing feeding patterns in this study, suggested by lower $\delta^{15}\text{N}$ values in acidified conditions, does not impair the capacity to source carbon environmentally or metabolically. The biomineralizing pathways of this species therefore appear robust even in potentially low-nutrient conditions triggered by OA. Ducker and Falkenberg (2020) investigated the metabolic and genetic response of *M. gigas* and observed no impacts on gene expression under OA conditions, suggesting that *M. gigas* is unlikely to experience metabolic alterations under OA on a broad physiological spectrum. However, the metabolic response of the oyster family should be investigated from a species-specific and temporal point. Parker et al. (2017) observed compromised aerobic metabolism under OA pCO_2 in *S. glomerata*. The study involved a 5 week-long acclimation period before altering water chemistry parameters. Thus, further investigations with longer treatments and different oyster species could highlight species-specific responses.

4.3. Environmentally $\delta^{13}\text{C}$ pathways

After comparing the two species in this study, the results from tissue and shell carbon suggest that the biomineralization response in *Mytilus* spp. differs to that in *M. gigas*. The shell $\delta^{13}\text{C}$ values in *M. gigas* do not suggest any altered biomineralization pathway under the treatment conditions, and extra feed does not significantly enhance metabolic uptake.

Although such a trend suggests a positive outcome for *M. gigas*, conversely, in *Mytilus* spp., decreasing pH causes an increase in environmentally sourced carbon for aragonite (Fig. 3). In *Mytilus* spp. a significantly lower $\delta^{13}\text{C}$ value following acidified seawater DIC below -1‰ indicating that CO_3^{2-} is the source of carbon from an environmental route into the shell (Fitzer et al., 2019a). In bivalves, environmental carbon sourcing tends to be the primary sequestration pathway, with seawater encountering gaps between the periostracum and the shell (McConnaughey and Gillikin, 2008). Although previous investigations found a metabolic response and acclimation to OA, in this study, OA affects shell $\delta^{13}\text{C}$ more than mantle carbon (Fig. 3). In addition, extra feeding does not significantly affect mantle or shell carbon uptake, suggesting that both species have physiological coping mechanisms to cope with OA. Indeed, the growth and hardness of both species was not affected by OA or extra food.

The $\delta^{13}\text{C}$ in *Mytilus* spp. aragonite and calcite results suggest that the effect of low pH causes variations between the two polymorphs, which react with opposing trends throughout the experimental treatments (Fig. 3). In shell calcite $\delta^{13}\text{C}$ values are higher under low pH, and warming causes a shift of carbon sourcing from HCO_3^- to CO_3^{2-} , which can result in reduced shell hardness, consequently, affecting the

biomineralizing pathway from seawater and food sourced carbon (Fitzer et al., 2014; Lee et al., 2021). This contrast relates to the important difference in the atomic configuration of the two polymorphs: calcite is a stable hexagonal form, while aragonite presents metastable orthorhombic crystals (Chandler, 2015). The marked difference between the two shell components in *Mytilus* spp. could indeed be linked to the energy cost of aragonite and calcite synthesis. Aragonite being more susceptible to OA-induced corrosion (Gazeau et al., 2007), may mean that more calcite could be produced than aragonite for the same energy cost. Similarly, Lee et al. (2021) observed that increased temperatures reduce carbon metabolic uptake into shell aragonite, while available biogenic calcite increases and under OA, molluscs rely on the least available e.g. carbonate CO_3^{2-} , rather than HCO_3^- (Lee et al., 2019), at detriment to growth. This adaptation might indeed be a sufficient adjustment to maintain control-level biomineralization in calcite but not in aragonite, as this is considered a more energetically costly polymorph (Fitzer et al., 2014; Huang and Zhang, 2022; Shi et al., 2019). In this study, while shell hardness is not affected by OA, the thickness of *Mytilus* spp. calcite layer responds to temperature increase (Fig. 4). The presence of thicker calcite shells may be a form of resilience to OA, increasing the structural strength, protecting body tissues against short-term exposure to warming. Indeed, in this study, $\delta^{13}\text{C}$ values increase in calcite but decrease in aragonite. This stands with the overall energy cost of biomineralizing two different polymorphs, and the difficulty of biomineralizing aragonite under OA. For example, carbon mobilised from the mantle would be reverted to calcite formation, rather than aragonite. Also, environmentally sourced carbon could be harder to recruit in aragonite shells, as crystallography configuration can be affected by elevated pCO_2 (Fitzer et al., 2014).

In *M. gigas* shell calcite biomineralization pathways for $\delta^{13}\text{C}$ uptake and mobilisation are not affected by OA in this study. Although *M. gigas* appears sensitive to pH alterations in terms of nitrogen uptake into mantle tissue and therefore altered feeding routine, this does not affect the shell growth or biomineralization pathway.

Finally, *Mytilus* spp. calcite also appear to be more resilient to low pH and high temperatures with change in carbon sourcing from a metabolic source compared to environmental source of carbon in the shell aragonite. Calcite biomineralization increases in conjunction with lower metabolically stored carbon at the cost of aragonite, which decreases significantly when calcite biomineralization is prioritised. On the other hand, *M. gigas* shows phenotypic plasticity to environmentally change under OA with continued growth with maintained biomineralization pathways. Both species show that extra feed is not a useful resource to counteract OA.

5. Conclusion

In conclusion, this study highlights the species-specific difference in OA-induced physiological responses within two mollusc species. Given that both *Mytilus* spp. and *M. gigas* biomineralize calcite shells, the pathways of biomineralization for the same CaCO_3 polymorph differ. *Mytilus* spp. appear to rely on metabolically sourced carbon for shell calcite potentially from extrapallial fluid rather than mantle tissue or from the feed under OA, and when seawater temperature rises. The altered biomineralization pathway in *Mytilus* spp. into the shell calcite layer, is sufficient to maintain the growth of the shell, as well as its thickness and hardness. On the other hand, *Mytilus* spp. increases environmentally sourced carbon for aragonite under low pH conditions. This response is sufficient to maintain and increase shell thickness in high water temperature scenarios. Low pH also affects *M. gigas* from a feeding and nutrient perspective shown by variation in mantle nitrogen isotopes, but biomineralization pathway is maintained along with growth. Thus, the response to OA and extra feeding results appear species-specific according to the carbon sourcing preference of *Mytilus* spp. and *M. gigas*. In a natural scenario, plankton blooms would be more beneficial to *M. gigas*, as in this study shows overall better shell

performance and resilience than *Mytilus* spp.

Funding

This project was supported by RCUK NERC Independent Research Fellowship funding [NE/N01409×/2] awarded to S. Fitzer.

CRediT authorship contribution statement

Isabella Mele: Investigation, Data curation, Formal analysis, Visualization, Writing – original draft, Writing – review & editing. **Rona A. R. McGill:** Supervision, Investigation, Data curation, Writing – review & editing. **Jordan Thompson:** Investigation, Data curation, Writing – review & editing. **James Fennell:** Investigation, Data curation, Writing – review & editing. **Susan Fitzer:** Conceptualization, Funding acquisition, Project administration, Methodology, Investigation, Visualization, Writing – review & editing.

Declaration of competing interest

The authors declare that they have no known competing financial interests or personal relationships that could have appeared to influence the work reported in this paper.

Data availability

All data has been provided in the supplementary materials.

Acknowledgments

The authors would like to thank Conor Drysdale, Simon Barnett, and Chessor Matthew for their support during experimental culture at the Marine Environmental Research Laboratory, University of Stirling in Machrihanish and Julie Dougans at the Scottish Universities Environment Research Centre (SUERC) for their support with carbon isotope sample preparation and analysis.

Appendix A. Supplementary data

Supplementary data to this article can be found online at <https://doi.org/10.1016/j.marenvres.2023.105925>.

References

- Bearhop, S., Adams, C.E., Waldron, S., Fuller, R.A., Macleod, H., 2004. Determining trophic niche width: a novel approach using stable isotope analysis. *J. Anim. Ecol.* 73 (5), 1007–1012.
- Beesley, A., Lowe, D.M., Pascoe, C.K., Widdicombe, S., 2008. Effects of CO₂-induced seawater acidification on the health of *Mytilus edulis*. *Clim. Res.* 37 (2–3), 215–225.
- Beniash, E., Ivanina, A., Lieb, N.S., Kurochkin, I., Sokolova, I.M., 2010. Elevated levels of carbon dioxide affect metabolism and shell formation in oysters *Crassostrea virginica*. *Mar. Ecol. Prog. Ser.* 419, 95–108.
- Carmichael, R.H., Shriver, A.C., Valiela, I., 2012. Bivalve response to estuarine eutrophication: the balance between enhanced food supply and habitat alterations. *J. Shellfish Res.* 31 (1), 1–11.
- Castillo, N., Saavedra, L.M., Vargas, C.A., Gallardo-Escárate, C., Détrée, C., 2017. Ocean acidification and pathogen exposure modulate the immune response of the edible mussel *Mytilus chilensis*. *Fish Shellfish Immunol.* 70, 149–155.
- Carboni, S., Evans, S., Tanner, K.E., Davie, A., Bekaert, M., Fitzer, S.C., 2021. Are shell strength phenotypic traits in mussels associated with species alone? *Aquaculture Journal* 1 (1), 3–13.
- Chandler, D., 2015. Mystery Solved: Why Seashells' Mineral Forms Differently in Seawater. MIT News. Available at: <https://news.mit.edu/2015/why-seashell-mineral-forms-differently-in-seawater-0302#:~:text=Calcium%20carbonate%20can%20take%20the,can%20ultimately%20transfo>. (Accessed 14 April 2022).
- Clark, M., 2020. Molecular mechanisms of biomineralization in marine invertebrates. *J. Exp. Biol.* 223 (11).
- Cole, M., Valiela, I., Kroeger, K., Tomasky, G., Cebrian, J., Wigand, C., McKinney, R., Grady, S., Carvalho da Silva, M., 2004. Assessment of a $\delta^{15}\text{N}$ isotopic method to indicate anthropogenic eutrophication in aquatic ecosystems. *J. Environ. Qual.* 33 (1), 124–132.
- Ducker, J., Falkenberg, L., 2020. How the Pacific oyster responds to ocean acidification: development and application of a meta-analysis based adverse outcome pathway. *Front. Mar. Sci.* 7.
- Feely, R.A., Sabine, C.L., Hernandez-Ayon, J.M., Ianson, D., Hales, B., 2008. Evidence for upwelling of corrosive "acidified" water onto the continental shelf. *Science* 320 (5882), 1490–1492. <https://doi.org/10.1126/science.1155676>.
- Fitzer, S., Phoenix, V., Cusack, M., Kamenos, N., 2014. Ocean acidification impacts *Mytilus* spp. control on biomineralisation. *Sci. Rep.* 4 (1).
- Fitzer, S.C., Zhu, W., Tanner, K.E., Phoenix, V.R., Kamenos, N.A., Cusack, M., 2015a. Ocean acidification alters the material properties of *Mytilus edulis* shells. *J. R. Soc. Interface* 12 (103), 20141227.
- Fitzer, S.C., Vittert, L., Bowman, A., Kamenos, N.A., Phoenix, V.R., Cusack, M., 2015b. Ocean acidification and temperature increase impact mussel shell shape and thickness: problematic for protection? *Ecol. Evol.* 5 (21), 4875–4884.
- Fitzer, S., Torres Gabarda, S., Daly, L., Hughes, B., Dove, M., O'Connor, W., Potts, J., Scanes, P., Byrne, M., 2018. Coastal acidification impacts on shell mineral structure of bivalve mollusks. *Ecol. Evol.* 8 (17), 8973–8984.
- Fitzer, S., McGill, R., Torres Gabarda, S., Hughes, B., Dove, M., O'Connor, W., Byrne, M., 2019a. Selectively bred oysters can alter their biomineralization pathways, promoting resilience to environmental acidification. *Global Change Biol.* 25 (12), 4105–4115.
- Fitzer, S., Plancq, J., Floyd, C., Kemp, F., Toney, J., 2019b. Increased pCO₂ changes the lipid production in important aquacultural feedstock algae *Isochrysis galbana*, but not in *Tetraselmis suecica*. *Aquaculture and Fisheries* 4 (4), 142–148.
- Freeman, A.S., Byers, J.E., 2006. Divergent induced responses to an invasive predator in marine mussel populations. *Science* 313, 831–833.
- Gazeau, F., Quiblier, C., Jansen, J., Gattuso, J., Middelburg, J., Heip, C., 2007. Impact of elevated CO₂ on shellfish calcification. *Geophys. Res. Lett.* 34 (7).
- Gaylord, B., Hill, T.M., Sanford, E., Lenz, E.A., Jacobs, L.A., Sato, K.N., Russell, A.D., Hettinger, A., 2011. Functional impacts of ocean acidification in an ecologically critical foundation species. *J. Exp. Biol.* 214 (15), 2586–2594.
- Hamm, L., Nakhoul, N., Hering-Smith, K., 2015. Acid-base homeostasis. *Clin. J. Am. Soc. Nephrol.* 10 (12), 2232–2242.
- Hettinger, A., Sanford, E., Hill, T., Hosfelt, J., Russell, A., Gaylord, B., 2013. The influence of food supply on the response of Olympia oysters larvae to ocean acidification. *Biogeosciences* 10 (10), 6629–6638.
- Hoegh-Guldberg, O., Cai, R., Poloczanska, E.S., Brewer, P.G., Sundby, S., Hilmi, K., Fabry, V.J., Jung, S., 2014. The Ocean. In: *Climate Change 2014: Impacts, Adaptation, and Vulnerability. Part B: Regional Aspects. Contribution of Working Group II to the Fifth Assessment Report of the Intergovernmental Panel on Climate Change (IPCC)*. Cambridge University Press, pp. 1655–1731.
- Howard, J.K., Cuffey, K.M., Solomon, M., 2005. Toward using *margaritifera falcata* as an indicator of base level nitrogen and carbon isotope ratios: insights from two California coast range rivers. *Hydrobiologia* 541 (1), 229–236.
- Huang, J., Zhang, R., 2022. The mineralization of Molluscan shells: Some unsolved problems and special considerations. *Front. Mar. Sci.* 9, 874534. <https://doi.org/10.3389/fmars.2022.874534>.
- IPCC, 2018. Global Warming of 1.5°C. An IPCC Special Report on the impacts of global warming of 1.5°C above pre-industrial levels and related global greenhouse gas emission pathways. In: Zhai, V.P., Pörtner, H.-O., Roberts, D., Skea, J., Shukla, P.R., Pirani, A., Moufouma-Okia, W., Péan, C., Pidcock, R., Connors, S., Matthews, J.B.R., Chen, Y., Zhou, X., Gomis, M.I., Lonnoy, E., Maycock, T., Tignor, M., Waterfield, T. (Eds.), *The Context of Strengthening the Global Response to the Threat of Climate Change, Sustainable Development, and Efforts to Eradicate Poverty* [Masson-Delmotte, Press.
- IPCC, 2021. In: Zhai, V.P., Pirani, A., Connors, S.L., Péan, C., Berger, S., Caud, N., Chen, Y., Goldfarb, L., Gomis, M.I., Huang, M., Leitzell, K., Lonnoy, E., Matthews, J.B.R., Maycock, T.K., Waterfield, T., Yelekçi, O., Yu, R., Zhou, B. (Eds.), *Climate Change 2021: the Physical Science Basis. Contribution of Working Group I to the Sixth Assessment Report of the Intergovernmental Panel on Climate Change* [Masson-Delmotte, Cambridge University Press, Cambridge, United Kingdom and New York, NY, USA.
- Jones, E.M., Fenton, M., Meredith, M.P., Clargo, N.M., Ossebaer, S., Ducklow, H.W., Venables, H.J., de Baar, H.J.W., 2017. Ocean acidification and calcium carbonate saturation status in the coastal zone of the West Antarctic Peninsula. *Deep Sea Res. Part II Top. Stud. Oceanogr.* 139, 181–194.
- Lafrancois, T., Fritts, A., Knights, B., Karns, B., 2018. Stable isotope comparison between mantle and foot issue of two freshwater unionids: implications for food web studies. *Freshwater Mollusk Biology and Conservation* 21, 28–35.
- Lake, J.L., McKinney, R.A., Osterman, F.A., Pruell, R.J., Kiddon, J., Ryba, S.A., Libby, A.D., 2001. Stable nitrogen isotopes as indicators of anthropogenic activities in small freshwater systems. *Can. J. Fish. Aquat. Sci.* 58 (5), 870–878.
- Lee, T., McGill, R., Fitzer, S., 2021. Effects of extra feeding combined with ocean acidification and increased temperature on the carbon isotope values ($\delta^{13}\text{C}$) in the mussel shell. *J. Exp. Mar. Biol. Ecol.* 541, 151562.
- Matoo, O., Lannig, G., Bock, C., Sokolova, I., 2021. Temperature but not ocean acidification affects energy metabolism and enzyme activities in the blue mussel *Mytilus edulis*. *Ecol. Evol.* 11 (7), 3366–3379.
- McConnaughey, T., Gillikin, D., 2008. Carbon isotopes in mollusk shell carbonates. *Geo Mar. Lett.* 28 (5–6), 287–299.
- Melzner, F., Stange, P., Trübenbach, K., Thomsen, J., Casties, I., Panknin, U., Gorb, S., Gutowska, M., 2011. Food supply and seawater pCO₂ impact calcification and internal shell dissolution in the blue mussel *Mytilus edulis*. *PLoS One* 6 (9), e24223.
- Montoya, J.P., 2007. Natural abundance of ^{15}N in marine planktonic ecosystems. In: Michener, R., Lajtha, K. (Eds.), *Stable Isotopes in Ecology and Environmental Science*, second ed. Blackwell Publishing Ltd.
- Pörtner, H.-O., 2008. Ecosystem effects of ocean acidification in times of ocean warming: a physiologist's view. *Mar. Ecol. Prog. Ser.* 373, 203–217.

- Patterson, H.K., Carmichael, R.H., 2018. Dissolved oxygen concentration affects d15N values in oyster tissues: implications for stable isotope ecology. *Ecosphere* 9 (3).
- Parker, L., Scanes, E., O'Connor, W., Coleman, R.A., Byrne, M., Pörtner, H.O., Ross, P.M., 2017. Ocean acidification narrows the acute thermal and salinity tolerance of the Sydney rock oyster *Saccostrea glomerata*. *Mar. Pollut. Bull.* 122, 263–271.
- Perkins, M.J., McDonald, R.A., van Veen, F.J.F., Kelly, S.D., Rees, G., Bearhop, S., 2014. Application of nitrogen and carbon stable isotopes ($\delta^{15}\text{N}$ and $\delta^{13}\text{C}$) to quantify food chain length and trophic structure. *PLoS One* 9 (3), e93281.
- Riebesell, U., Fabry, V.J., Hansson, L., Gattuso, J.P., 2010. Guide to Best Practices for Ocean Acidification Research and Data Reporting. Directorate General for Data Reporting, European Commission.
- Robinson, D., 2001. $\delta^{15}\text{N}$ as an integrator of the nitrogen cycle. *Trends Ecol. Evol.* 16 (3), 153–162.
- Sanders, T., Schmittmann, L., Nascimento-Schulze, J., Melzner, F., 2018. High calcification costs limit mussel growth at low salinity. *Front. Mar. Sci.* 5.
- Shi, T., Wang, Y., Zhao, Y., Loucaides, S., 2019. Detecting the calcium carbonate saturation state under the stress of ocean acidification using saturometry technique. *IOP Conf. Ser. Earth Environ. Sci.* 227.
- Thomsen, J., Casties, I., Pansch, C., Körtzinger, A., Melzner, F., 2013. Food availability outweighs ocean acidification effects in juvenile *Mytilus edulis*: laboratory and field experiments. *Global Change Biol.* 19 (4), 1017–1027.
- Tomanek, L., Zuzow, M.J., Ivanina, A.V., Beniash, E., Sokolova, I.M., 2011. Proteomic response to elevated PCO_2 level in eastern *M. gigas*, *Crassostrea virginica*: evidence for oxidative stress. *J. Exp. Biol.* 214, 1836–1844.
- Waldbusser, G., Hales, B., Haley, B., 2015. Calcium carbonate saturation state: on myths and this or that stories. *ICES (Int. Counc. Explor. Sea) J. Mar. Sci.* 73 (3), 563–568.
- Wijsman, J., Troost, K., Fang, J., Roncarati, A., 2018. Global Production of Marine Bivalves. Trends and Challenges. *Goods And Services Of Marine Bivalves*, pp. 7–26.